Nanoscale

RSCPublishing

PAPER

View Article Online
View Journal | View Issue



# Next-generation nanotechnology laboratories with simultaneous reduction of all relevant disturbances

Cite this: *Nanoscale*, 2013, **5**, 10542

Emanuel Lörtscher,* Daniel Widmer and Bernd Gotsmann

Received 1st July 2013
Accepted 12th August 2013

DOI: 10.1039/c3nr03373b

www.rsc.org/nanoscale

The tremendous variety of nanotechnology experiments and tools to fabricate and characterize ever-smaller structures down to molecular or even atomic scales leads to stringent demands for appropriate, so-called "silent", premises that allow such susceptible experiments to be conducted. Reducing dimensions means smaller absolute optical and electrical signal levels, and consequently reduced signal-to-noise ratios. Hence, in addition to short-range disturbances inside the laboratory, remote long-range noise sources have to be considered for next-generation laboratories that aim at screening the disturbances and keeping the remaining values at utmost constancy. We present a novel laboratory concept that addresses simultaneously all the disturbances relevant for nanotechnology, namely, vibrations, electro-magnetic fields, temperature, humidity, and sound. Particular attention was paid to tackling the mutual derogation of the various measures to enable unprecedented performance of the novel research platform.

## 1. Introduction

Nanotechnology is related to dimensions smaller than 100 nm, and often deals with molecular (1–5 nm) or even atomic scales (< 1 nm). Both top-down and bottom-up fabrication of tiny devices require highly optimized equipment. Nanotechnology experiments can be extremely challenging in terms of positioning accuracy, deflection of the image-producing beam (electron or ion beam) or probe (scanning tunneling microscope, atomic force microscope) at generally low signal levels. There are numerous types of internal interferences and external disturbances that affect experimental results; temperature-induced drifts make long-term investigations impossible because of the relative motion between probe and sample, or external electro-magnetic stray fields deflect charged particle beams, such as an electron or ion beam. Commercial tools used for cutting-edge nanoscale fabrication and characterization, such as electron-beam lithography (EBL), transmission electron microscopes (TEM) or focused ion-beam (FIB) tools, frequently require optimized laboratories that are sufficiently "silent" to achieve the performance guaranteed. Often, these demanding room specifications can hardly be achieved in standard buildings, resulting in a major performance loss and limited applications. In the framework of the Binnig and Rohrer Nanotechnology Center (BRNC), built as a strategic partnership between IBM Research, Zurich and the Swiss Federal Institute for Technology Zurich (ETHZ), a construction volume was reserved for novel research laboratories dedicated to the most sensitive fabrication and characterization of nanostructures. The building site is non-ideally situated above ground between a motorway and two streets (20–120 m in distance), and is crossed underground by a railway tunnel (180 m in distance) (see Fig. 1a) – obviously a very challenging site to achieve low-noise laboratories because of seismic vibrations and vagrancy return currents (at the railway frequency of 16.7 Hz). The main target for the design of the laboratories was to achieve a simultaneous reduction of all disturbances relevant for nanotechnology originating from external (Fig. 1a) and internal (Fig. 1b) sources, rather than to achieve only one outstanding value for one specific noise source.

Given the manifold room requirements of state-of-the-art research tools, we considered the following disturbances as relevant for nanotechnology: any kind of mechanical vibration, electro-magnetic fields, temperature gradients, humidity changes, and acoustic noise. For every one of those disturbances alone, known measures exist that can lead to significant improvements compared with "normal" ambient levels. Impressive examples are, *e.g.*, the magnetically most silent room[1] with screening factors of more than 100 and remaining fields of less than 0.5 nT or the acoustically most quiet room[2] with sound levels of −9.4 dBA. The simultaneous reduction of all disturbances in one room, however, constitutes a much more complex situation and requires careful analysis of the mutual derogation of the technically known measures, in particular if the room should still be accessible and easy to equip. Here, we propose a novel laboratory concept[3] that was planned and tested intensively for three years. Six labs were finally realized, ranging from 25 $m^2$ to 50 $m^2$ floor area at a room height of 6.8 m each. The laboratory concept as sketched in Fig. 2 will be presented in detail in the following.

*IBM Research – Zurich, Säumerstrasse 4, CH-8803 Rüschlikon, Switzerland. E-mail: eml@zurich.ibm.com; Fax: +41 44 724 89 58; Tel: +41 44 724 89 74*

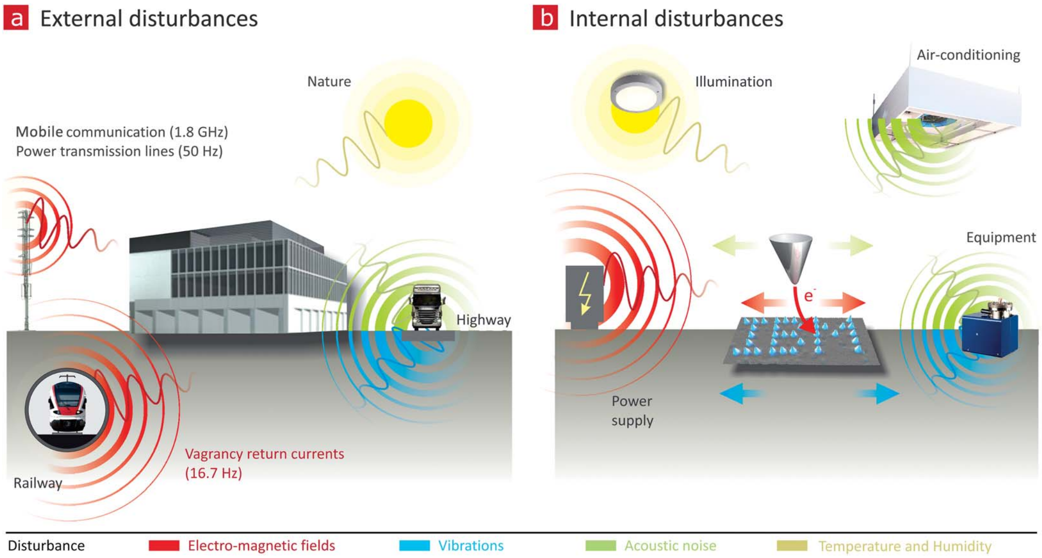


**Fig. 1** Non-exhaustive illustration of the various disturbances at the laboratory site: (a) building-external disturbances generally depend on the civilization factor, such as streets, railways, mobile communications, *etc.*, and natural environmental conditions. (b) Lab-internally generated disturbances originate from equipment or building installations as well as from the operator and instrumentation.



## 2. Floor vibrations

Nanotechnology experiments often rely on the precise positioning of a probe with respect to a defined position on a sample (such as the tip of a scanning probe microscope or the electron beam in a scanning electron microscope). The desired accuracy ranges from some tens of nanometers down to sub-atomic dimensions. Vibrations (as well as temperature drifts and electro-magnetic deflections; see below) may induce varying internal displacements in devices. To some extent, they can be minimized by appropriate design of the experimental system. For the highest accuracy levels, however, external excitation of the mechanical degrees of freedom can become critical, in particular where floor vibrations or acoustic excitations are concerned. Fig. 3a shows floor-vibration levels for various types of rooms ranging from offices to rooms meeting vibration criterion (VC) standards VC-A to VC-E[4] and the most recently added VC-F and -G curves.[5] Also shown are NIST-A and NIST-A1 recommendations achieved in the Advanced Measurement Laboratories of the National Institute of Standards and Technology (NIST) in Gaithersburg.[5]

As mentioned, the main sources of floor vibrations frequently lie outside the building. A nearby motorway and a nearby railway were identified as main excitation sources. The sub-optimal[6] site location in terms of remote seismic ground excitations was taken into account when laying down the building foundation directly on the bedrock (molasse conglomerate). This basically couples the building's basement to the tremendous mass of the underlying bedrock, making it almost impossible for remote sources to excite the underground because of the large mass imbalance between excitation source and bedrock. Hence, in the laboratories located 8 m below ground level, only building-internal seismic excitations had to be considered. The vibration level measured on the bottom slab of the building was found to be already below the NIST-A1 specs (light gray dotted curve in Fig. 3a). The remaining floor vibrations measured stem from excitations inside the building, such as elevators, pumps, air-conditioning, humans, *etc.* As these disturbances typically occur when the equipment is close to the experimental setup, a spatial separation was introduced: a separate room is attached to every lab for housing auxiliary equipment such as pumps, transformers, chillers, *etc.* (see Fig. 2b and c).

To reduce the vibration levels further, additional measures were required. Typically two types of vibration-isolation systems are used. One type, as realized in standard optical tables, consists of placing the equipment on a table with a heavy top that is placed on springs, typically using compressed air. Such a spring-mass system is efficient for reducing any mechanical transmission above its mechanical resonance, typically tuned to be on the order of 1–10 Hz. The second strategy is to use active control by measuring incident vibrations acting on the setup and actively compensating them by means of electro-mechanical actuators. Both types of systems can achieve vibration levels below 10 $\mu m\ s^{-1}$ for vibrations not exceeding typical building amplitudes on the test bed's location. To go beyond these levels, a synergetic combination of the two approaches is required. Here, a heavy slab (labelled "main base" in Fig. 2b) was maximized in terms of mass such that its volume fills almost the entire room underneath the floor level. Depending on the desired frequency range, two distinctly different vibration damping systems were installed, where the bases sit on either air springs in combination with air cushions (System 1) or only air springs (System 2) (Fig. 2b and d). Active vibration control is implemented in System 1 using air springs, whereas System 2 uses electric actuators. In any case, for vibration level targets below 1 $\mu m\ s^{-1}$, it is necessary to understand which kind of vibrational excitations, other than those through the floor,

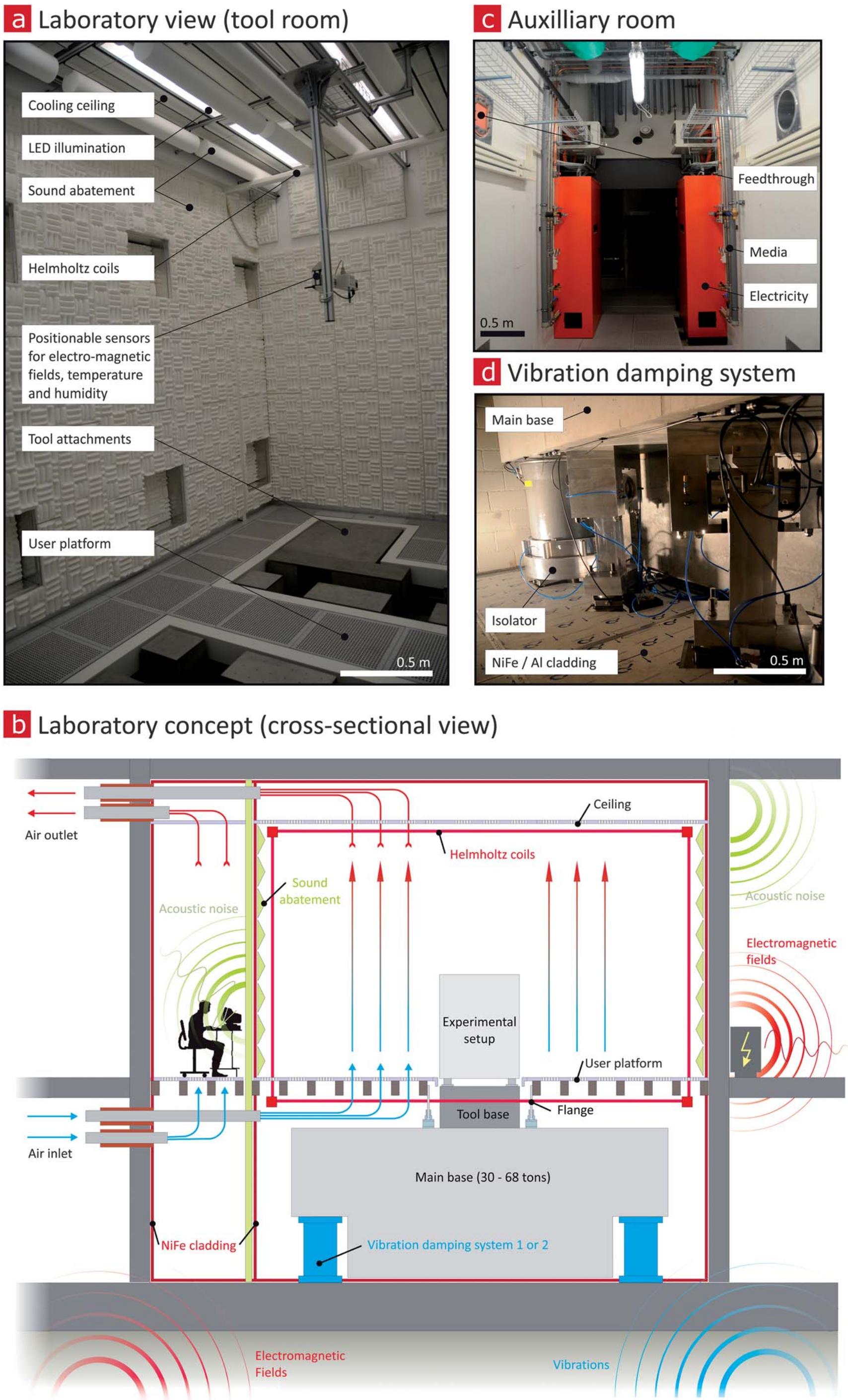


**Fig. 2** Details of the laboratory concept: (a) view of a small-sized lab with a floor area of approx. 25 m$^2$ prior to tool installation. (b) Schematic cross-sectional view of the lab including underground installations. (c) Partial view of the auxiliary room with media connections. (d) Vibration-damping system based on air springs and air cushions.

actuates the base because the soft suspension renders the base sensitive to the smallest excitations despite its heavy mass. The relevant actuation sources are air-flow from the air-conditioning system and interactions of humans. Both influences required special attention. As a consequence, the operator floor was separately suspended from the base and attached to the inner wall without any mechanical connection to the slab (Fig. 2b). The air-conditioning system, as described below, was designed in such a way that no air-flow can excite the base.

In the vibration-damping systems realized here, concrete slabs weighing between 30 and 68 tons (depending on the lab footprint) were chosen (mass without tools). The resonant frequencies of the resulting spring-mass systems were typically well below 5 Hz, which leads to passive rejection of mechanical

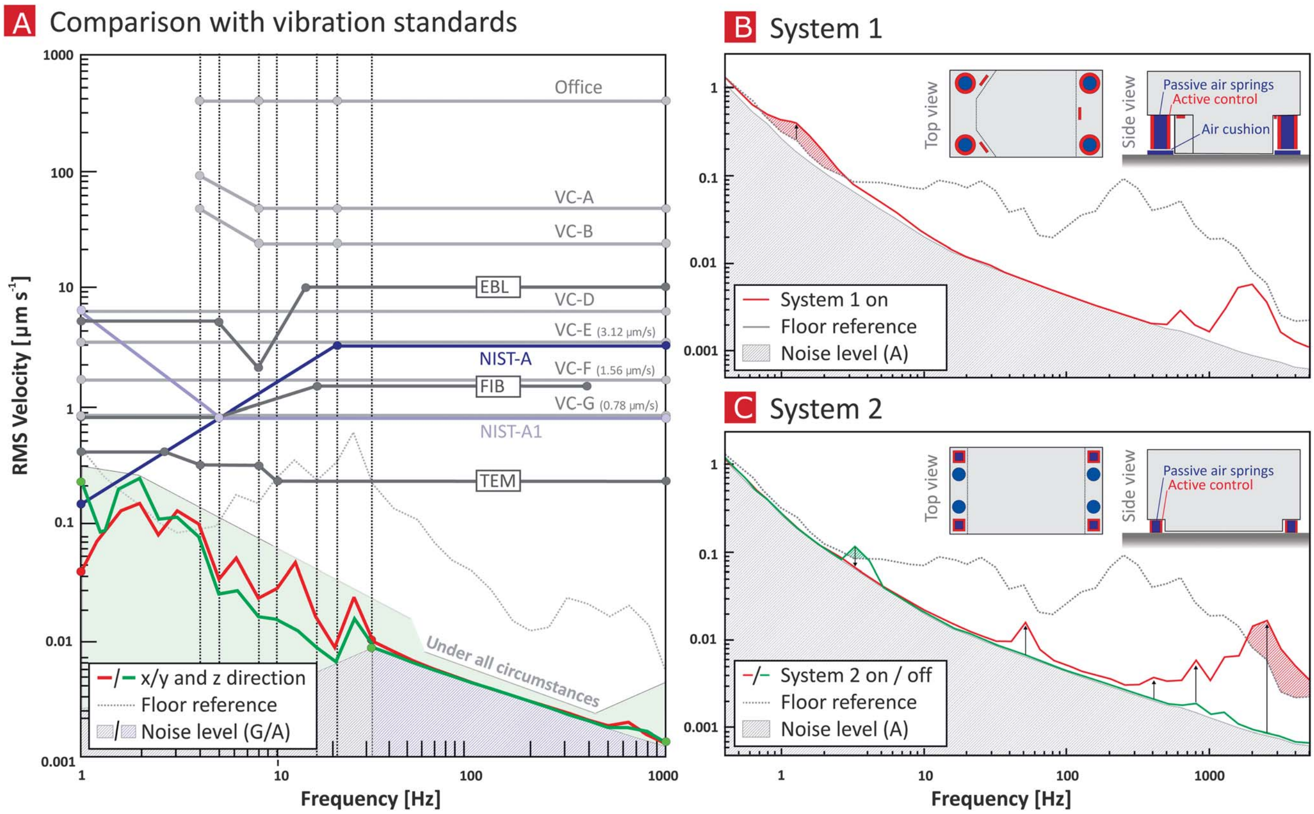


**Fig. 3** (a) Vibration levels measured in the lab in comparison to standards, tool requirements and references: IEST standards VC-A to VC-G (light gray), specs achieved at the NIST called NIST-A (dark blue) and NIST-A1 (light blue), typical room requirements of EBL, FIB and TEM tools (dark gray). Achieved vibration damping in the *x*/*y* (red) and *z* (green) directions on the suspended base (higher velocity of the two systems) compared with the floor reference (light gray dotted line). (b) System 1 (red) in comparison to simultaneously measured floor vibrations (light-gray dotted line) and sensor noise level (accelerometer). (c) System 2 with (red) and without (green) active control in comparison to simultaneously measured floor vibrations (light-gray dotted line) and sensor noise level (accelerometer). Lower (green) and higher (red) frequency ranges with respect to floor reference are indicated by shaded areas.

vibrations at higher frequencies. Active control is then used to reduce the remaining vibration amplitude, mainly at resonance and up to about 30 Hz. To achieve active control, the two systems use different strategies. System 1 uses relatively gentle control as known from vibration isolation at the source, reducing the vibration amplitudes at resonance by a factor of approx. 2. System 2, in contrast, uses a larger force response to suppress the low-frequency vibrations by a factor of approx. 10. In the latter case, however, mechanical excitations at frequencies around 50 Hz and higher are inevitable as the concrete base is not infinitely rigid. The vibrational modes excited start therefore with the lowest bending mode (torsional mode) of the concrete slab at 328 Hz and range into the kilohertz regime, whereas the 50 Hz peak is due to electro-magnetic contributions from the power supply. Frequencies above 100 Hz are of special concern because cutting-edge research tools require vibration control in the range from hundreds of Hz up to 1 kHz (see room requirements in Fig. 3a).

In general, to characterize vibration-damping systems, the response of the isolated slab to external excitations is measured in compliance and transmissibility curves. Both require a frequency-dependent force load to determine the spectral range over which the slab acts as a rigid body and to describe the damping of the system. As the weights involved are huge and well coupled to bedrock, excitations of the floor are difficult to achieve, hence measurements have to be conducted with respect to the floor vibrations.[7] The vibration spectrum of the floor strongly depends on the time of day, such that long-term measurements of floor *vs.* slab yield an almost complete excitation range. Fig. 3a shows floor-vibration data recorded in the daytime during normal working-day operation using System 1. The data show the RMS velocity in a third-octave bandwidth recorded with a velocity sensor (for a frequency range from 0.1 Hz to 30 Hz) and with an accelerometer (30 Hz to 1 kHz). The sensors were placed in the middle of the concrete slab surface. Between 30 Hz and 400 Hz, the vibration level is below the noise level of the measurement sensor. For frequencies above 10 Hz, a reduction of the vibration velocities on the order of one decade is observed. At the fundamental resonant frequencies of the slab-spring system at 1–3 Hz, System 1 reaches similar vibration values as the floor reference for *x*/*y* (red curve) and slightly higher values for the *z* axis (green curve in Fig. 3a). Above 4 Hz, the vibrations on the slab are much lower than the reference. The vibration levels obtained here are lower over the entire frequency range than those achieved in the Birck Nanotechnology Center at Purdue University,[8] published data from the NIST labs,[9] and levels in the "quietest building in the world" at the Bristol Center for Nanoscience and Quantum Information.[10]

The differences between the two damping systems become apparent from the frequency spectra shown in Fig. 3b (System 1) and Fig. 3c (System 2). Data are shown for the horizontal (the higher velocity for $x$ or $y$) and vertical directions ($z$) obtained on different days. The closed-loop control of System 2 (Fig. 3c) can be switched off so that the influence of active position control can be distinguished from the passive shielding through the spring-mass system alone. The fundamental resonance at 2.5 Hz is completely suppressed by the actuation system (green hatched area). However, the strong control effort induces vibrations at higher frequencies (50 Hz and larger) that may even exceed the floor reference (above 2 kHz; red hatched area). System 1, on the other hand, is tuned in such a way that the fundamental resonance of the spring-mass system is not completely suppressed. Consequently, at resonance ($\approx$1.5 Hz), the vibration amplitude is larger than the one of the floor reference (red hatched area in Fig. 3b) even while the system is active. At higher frequencies, however, the more gentle operation induces less vibration and exhibits smaller vibration levels than the floor reference in contrast to System 2. Which of the two systems is preferred depends on the experimental setup, in particular on the resonant frequencies of internal vibrations in the tools and the mounting of the tools on the concrete slab. We decided to implement both systems to have the most flexibility for the tooling planned.

## 3. Electromagnetic fields

Besides reducing and preventing vibrations, an efficient screening of electromagnetic fields (EMF) at 16.7 Hz railway frequency and 50 Hz power-supply frequency (as well as their harmonics) was another important task for the lab concept. The use of magnetic material to form a magnetic cage that screens low- and mid-frequency components (100 Hz – 100 kHz) is an established, but quite expensive solution. Technically challenging, however, was the fact that the magnetic cage should also enclose lab-internal components, such as the heavy main bases, user platform, ceiling, *etc.* (Fig. 2b) because the goal of every magnetic cage is to have as few openings as possible. The concept therefore uses an inner room inside the magnetic cage, to which the user platform, ceiling, *etc.* are attached. Thereby no holes had to be drilled into the magnetic material as any hole would weaken the screening efficiency. In addition to openings, also a high mechanical load acting on the magnetic sheets is detrimental to the screening efficiency as mechanical pressure decreases the relative permeability from 10 000 (soft-annealed magnetic material) – 100 000 (last stage of annealing) to just a few 100s. Hence, to cast the vibration-isolated bases, four wedge shoes were used to carry the boarding weight over local openings in the magnetic cage that can be closed with inlet sheets after striking and installation of the vibration-isolation system. These few and re-closable openings in the cage enabled highest point loads during the casting period. Moreover, also any door, air-conditioning channels (up to 1.5 m from the lab) and feedthroughs were coated with the magnetic material.

Single-layer sheets of isotropically conducting NiFe (80% Ni, 20% Fe) with a thickness of 350 μm and a soft-annealed permeability of 12 000 (saturation density 0.8 T) were used to coat the floor, walls and ceiling with 20 cm overlap at sheet borders. To clamp the sheets to the wall, a 2 mm-thick Al top layer protecting the NiFe from corrosion was seamlessly welded to create a Faraday cage for electric fields in addition to the magnetic screening. The use of additional NiFe layers would clearly increase the screening down to ultra-low levels,[11] but also reduce the usable lab volume and increase costs drastically. Fig. 4b shows the screening factors for the DC and low-frequency range up to 150 Hz for one and two layers of NiFe. In addition to the volume reduction when using multiple layers, the equipment in the lab will again be generating EMFs, hence the single-layer decision was a trade-off between an efficient screening and the prospective fields produced by lab-internal equipment.

The magnetic field of the Earth of 43 μT at the building site is reduced to 34–36 μT on the laboratory ground level by the heavy iron armoring of the building's basement. Inside the NiFe cladding of every lab, the DC field strength is reduced further, reaching values between 9 and 15 μT. Because of the repulsion of the Earth's magnetic field by the magnetic cages, high field concentrations are measured directly on or in close proximity to the NiFe layers (both inside or outside the cladding), especially in the vertical direction (60–140 μT). This indicates that the magnetic material is in saturation. The use of non-magnetic materials inside the laboratory, *e.g.*, glass-fiber-induced reinforcement of the suspended base and the inner walls to avoid magnetic induction, resulted in DC field distributions inside the labs that are homogeneous and vary only by $\pm$0.5 μT (in more than 15 cm distance to the cladding). An additional, smaller NiFe cladding around the core structure of the experimental setup reduces the DC component further with screening factors of up to 20 (Fig. 4b), reaching remaining DC fields below 1 μT inside the additional cladding.

In most experiments, a stable DC offset can be accounted for, but DC variations can be detrimental, *e.g.*, for EBL, TEM or FIB. Outside the laboratories, DC variations typically range between 400 and 5000 nT (blue curve in Fig. 4c) on very long time scales, *i.e.*, minutes or hours. Because of the long-range characteristics, it is difficult to identify the sources or to find possible counter measures. Given the saturation of the NiFe layer, the additional DC screening required for these variations is expected to be rather small. Hence, an additional active EMF cancellation system[12] installed inside the passive screening cage and based on three pairs of Helmholtz coils for every spatial direction was implemented and optimized in terms of the distance to the NiFe cladding to achieve the largest compensation volume for homogeneous field distributions. The system can control either up to 11 distinct frequencies (with individual PID parameters) or broadband up to 10 kHz. In our case, the first setting enables large gains to be set for the DC component and smaller ones for the AC components. Fig. 4a shows the passive screening of the NiFe cladding with and without the EMF cancellation system activated (red *vs.* black curve) with respect to the simultaneously

 

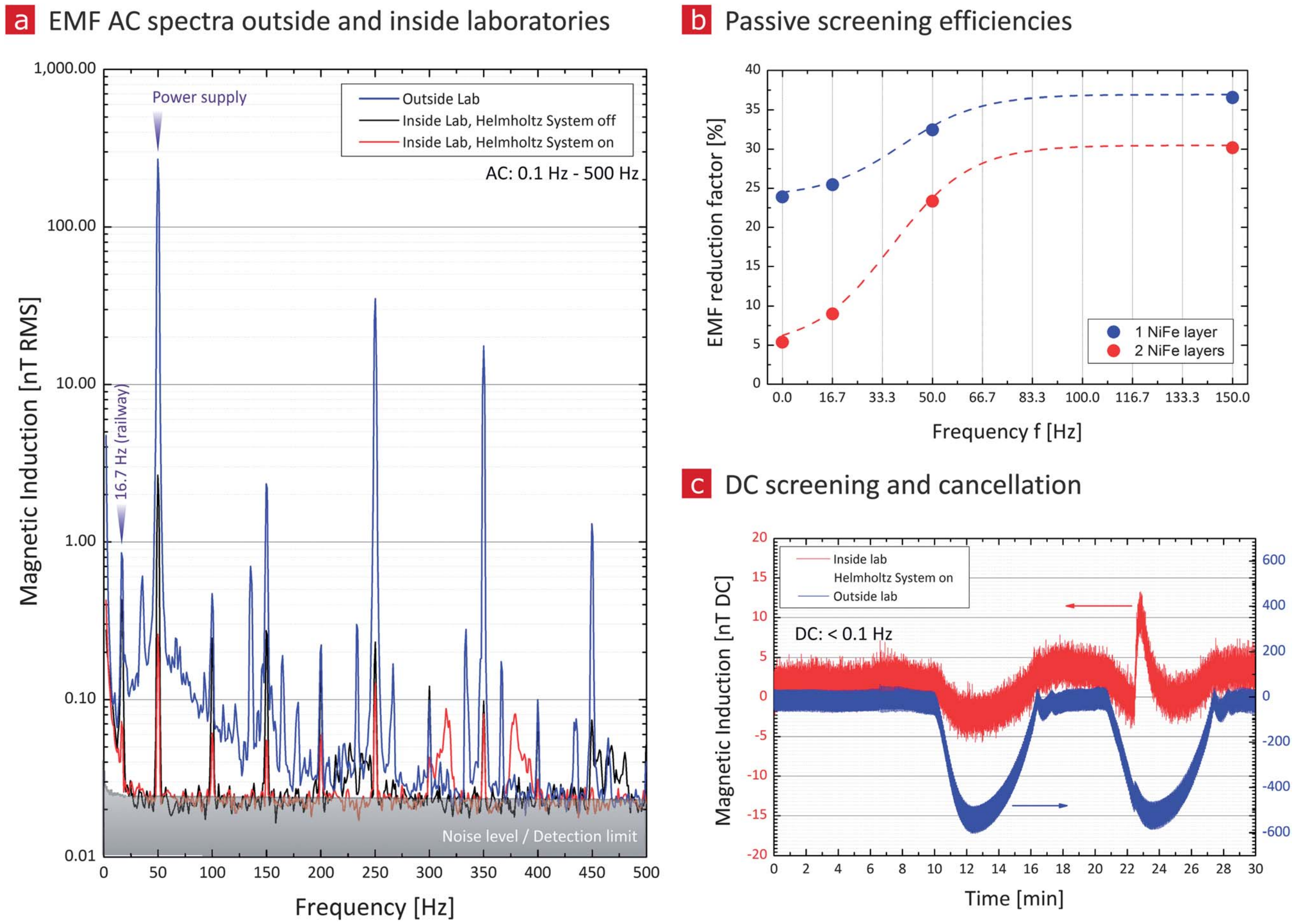


**Fig. 4** (a) EMF screening of the low-frequency AC components inside and outside the magnetically shielded labs from 0.1 Hz to 500 Hz. (b) Screening factors for one and two layers of NiFe (as measured by additional smaller cages inside the lab), and (c) active cancellation of the DC component by the active Helmholtz coil system.

measured EMF outside the lab (blue curve) for the frequency range from 0.1 to 500 Hz. The most dominant 50 Hz power line peak with 200–500 nT outside the lab is reduced by two orders of magnitude by the passive screening, and another order of magnitude by the active cancellation. The 3rd, 5th and 7th harmonics represent the second highest peaks and are all reduced in a similar way as the 50 Hz component by the passive screening. The side bands of the odd harmonics result from frequency static converters and are fully screened by the magnetic cage. The passive screening of the low-frequency 16.7 Hz railway component is very small (20–50%), and only the cancellation system is able to reduce it to below 0.1 nT. The system reduces efficiently 2nd, 3rd and 4th harmonics by at least one order of magnitude but at the cost of two satellite peaks for the 7th harmonic. For the DC component, the active cancellation performance is shown separately in Fig. 4c. Ultimately, and nota bene, when all other measures are active (vibration-isolation systems, air-conditioning, *etc.*), magnetic field strengths of clearly less than 0.2 nT peak-to-peak for 50 and 250 Hz and less than 0.1 nT peak-to-peak for other components were achieved. The variations of the DC component were found to be less than ±20 nT (Fig. 4c), guaranteeing negligible beam deflections for charged beams applications, such as SEM, TEM or FIB.

## 4. Temperature and humidity

Stable temperature and humidity conditions are usually achieved by exchange of large quantities of air. This approach is used in cleanrooms. Its implementation in low-noise rooms, however, would heavily affect other measures, *e.g.*, by exciting a softly suspended base by air streams, by air pressure acting directly on the experimental platforms, or simply by generating too much acoustic noise. Our concept depicted in Fig. 2b uses an upward-flow air-conditioning system (ACS), by which conditioned air is injected underneath the user platform, slightly above the sensitive main base. The perforated floor plates use semi-permeable membranes to achieve a homogeneous pressure distribution over the entire floor, and more importantly, also very close to the experiment (Fig. 2b). Moreover, the air-flow is vertical because of a pressure difference between inlet and outlet of 20 mPa. In contrast to standard top-down ACS, here the upward nonturbulent airstream aligns with the direction of the rising warm air stemming from the experimental setup, thereby reducing the turbulence. The incoming air is purified in an ACS system located approx. 5–25 m away from the labs and cooled to 0.25 °C below the set point. Separate air-flow and control circuits are used for the experiment and the operator room

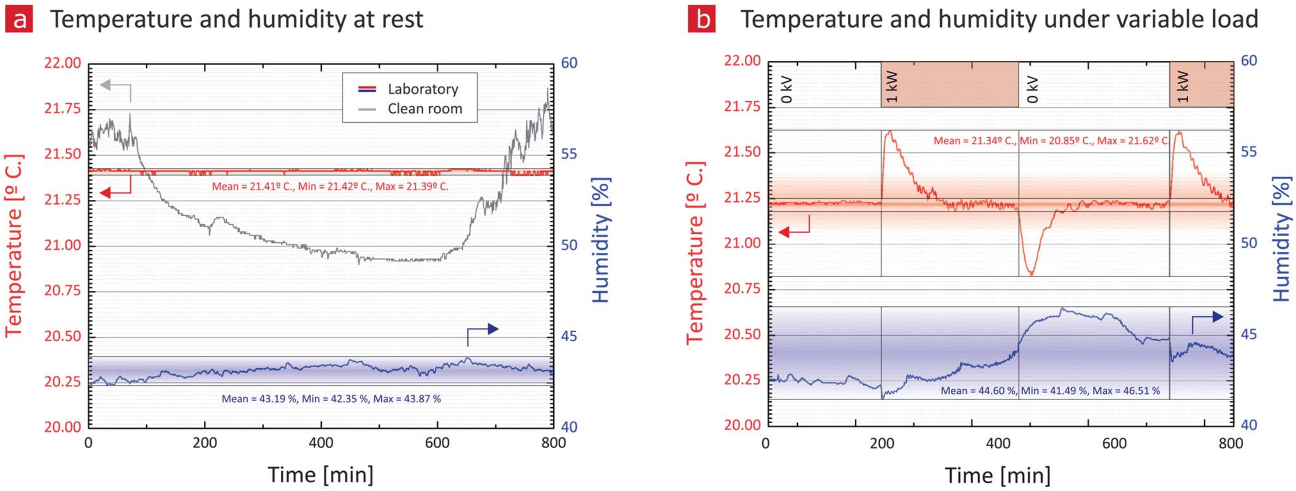


**Fig. 5** (a) Temperature and humidity stability at rest (closed door, constant heat load) and (b) with a variable load of 1 kW (in respect to 0 kW).

(see Fig. 2b). Local heater coils at the entrance adjust the temperature with utmost accuracy and no delay. A drawback of the inverted ACS is the circulation of any dust particles brought into the room, essentially an issue for processes requiring cleanroom class ISO 5 or better. This issue was solved by additional enclosures around the load-lock areas. Other than that, the nonturbulent ACS system is characterized by its low sound emission of only approx. 21 dBC at the air outlet, a value that is achieved in cutting-edge facilities only with the air-conditioning turned off.[13] Furthermore, the use of the entire floor for ventilation renders the ACS very efficient and laminar.

At rest (closed doors, constant heat load of approx. 1.2 ± 0.2 kW), we achieve an absolute temperature stability of ±0.01 °C in the labs (at an average temperature of 21.42 °C for a set point of 21.50 °C). Typical temperature profiles are shown in Fig. 5a (red curve) and compared with data measured in the same period of time in our cleanroom facility with a temperature stability of ±0.5 °C (light-gray curve). In the same period of time, the humidity varies between 42 and 44%. The heat load inside the lab is expected to be quite constant as the heat-generating equipment with variable load is located in the adjacent auxiliary rooms. The ACS performance for variable load can be demonstrated by placing heaters directly underneath the master sensor. The abrupt power-on of 1 kW thermal heat increases the temperature by +0.42 °C, which then relaxes slowly (within 90 min) to its initial set point owing to the inertial control parameters. The fluctuations of ±0.025 °C when returning to the set point stem from fluctuations in the heating power of the electrical oven. When the heater is switched off, a dip in the temperature profile of −0.43 °C occurs because of (a) the slow PID settings and (b) the latent cooling power in the additional cooling ceiling installed (Fig. 2b). To summarize, the air-conditioning achieves a superior absolute temperature stability of ±0.01 °C with very little sound emission (<21 dBC) and negligible excitation of the vibration damping system (no difference observable in vibration spectra when ACS is on or off).

## 5. Additional measures

In addition to the novel system components developed specifically for this project described above, standard components for low-noise rooms were used. For instance, we used sound-absorbing elements to coat the walls entirely and the ceiling partially. These will absorb acoustic noise generated by the experimental setup itself. The lighting is based on a high-efficient LED illumination with remote DC power supply so as not to disturb the electromagnetic parameters during set up of the experiments (experiments are usually performed in complete darkness). Tool bases are designed individually for every tool footprint, using stainless-steel attachments for force-fit manner connections of the tool to the heavy main base. All parameters of the vibration-damping system, the active Helmholtz coil system, and temperature and humidity control can be tuned and are adjusted to the specific tools and experiments individually. All environmental parameters of every room are logged by a server application to correlate experimental results and possible remaining disturbances. Finally, to benefit fully from the excellent room performance, remote control (from the operator room as depicted in Fig. 2b or farther away in the building) for all experiments is key to undisturbed experiments and excellent results.

## 6. Conclusions

In summary, the novel laboratory concept reduces all relevant disturbances for fabrication and characterization simultaneously to unprecedentedly low levels with the smallest fluctuations. We achieve vibrations of less than 300 nm $s^{-1}$ at 1 Hz and less than 10 nm $s^{-1}$ above 100 Hz; electromagnetic fields with AC peaks of less than 0.3 nT at 50 Hz and 250 Hz; and DC variations of less than ±15 nT. Furthermore, the temperature is kept constant within ±0.01 °C and the humidity within ±2%. Acoustic noise is below 21 dBC. The cost for this performance is estimated to be approx. 1.5 Mio CHF/lab (or approx. 45 000 CHF $m^{-2}$ in comparison with approx. 3000 CHF $m^{-2}$ for class

100 (ISO 5) clean rooms). The number includes design, construction and fabrication with all components in case the labs can be planned simultaneously with the rest of the building. The novel research platform established and tested comprehensively allows extremely sensitive experiments to be conducted with higher accuracy and over a longer time. Cutting-edge commercial tools are no longer limited in their performance by environmental disturbances. In general, the generic concept proposed is flexible and allows further extension of the measures implemented to achieve the ultimate performance. These strategies include adding combinations of passive and active electromagnetic screening layers, increasing the mass of the suspended base, building local climate enclosures with radiation cooling and/or installing more sound-absorbing and scattering measures. In that sense, the laboratory concept is believed to ultimately enable entirely novel experiments and applications, going far beyond the initial nanotechnology demand.

## Experimental section

### Methods

The laboratories' performances were characterized in-house using our own equipment and in addition by independent companies which were not involved in either the planning or the realization process to guarantee an objective, certified characterization.

### Vibration measurements

A Brüel and Kjaer Seismic IEPE Accelerometer with a sensitivity of 10 V $g^{-1}$ and a triaxial IEPE Accelerometer with a sensitivity of 1 V $g^{-1}$ were used. Third-octave bandwidth velocity spectra were obtained after Fourier transform of the raw data (data acquisition with ADwin by Jaeger Messtechnik, Germany) and the application of a digital filter following DIN 45652. In addition, MR2002 and MS2003+ by Syscom, Switzerland, and data analysis software by Ziegler Consultants, Zurich, were used.

### Electro-magnetic measurements

Bartington Three-Axis Magnetic Field sensors Mag-03 type "low-noise" were employed. The noise-level is measured only up to 10 Hz and estimated as shown in Fig. 4a according to specification (noise < 6pTrms/$\sqrt{}$Hz at 1 Hz). Data acquisition was performed using a Bartington Spectramag-6 unit with data recording rates of 10 kHz.

### Temperature measurements

Ellab TrackSense Pro-X data loggers with PT1000 temperature sensors with a measurement accuracy of $\pm 0.005°$ were employed.

## Author contribution

E.L. coordinated and headed the project. B.G. conducted vibrational measurements. E.L. conducted electromagnetic and temperature measurements. E.L. and D.W. were responsible for the room layout. D.W. was responsible for the auxiliary rooms, supported all installations and developed server applications for data logging. E.L., D.W. and B.G. analyzed the data and wrote the paper. The realization of the laboratory site was conducted by more than 35 companies under a total services contractor.

## Acknowledgements

We are grateful to W. Riess, R. Germann, S. Blunier, U. Dürig, R. Allenspach, A. Bischof, and E. Wyss for technical and scientific discussions. We appreciated the strategic and financial support from J. Kelly III, M. Kaiserswerth, P. Seidler, T. Schlund, M. Idda, and R. Schneider. We are very grateful to the following people from the companies involved in the planning and construction of the entire building (in alphabetic order): P. Büchel, M. Bapst, L. Beck, M. Biondi, H. Edbauer, R. Fässler, M. Geeler, R. Hauri, P. Heiland, T. Huber, G. Hugelshofer, P. Keller, R. Krieg, J. Kryenbühl, H. Mühlematter, H. Meierhofer, U. Moser, U. Motz, U. Pedraita, H. Roman, J. Schmidt, and. H. Seifert.

## References

1 Physikalisch-Technische Bundesanstalt (PTB), Institut Berlin.
2 Orfield Laboratories.
3 E. Lörtscher, B. Gotsmann, D. Widmer and U. Dürig, CH920110032ep1, 2011.
4 *Generic Criteria for Vibration-Sensitive Equipment*, 1991.
5 H. Amick, M. Gendreau, T. Busch, and C. Gordon *Evolving criteria for research facilities: vibration, Proceedings of PIE Conference 5933*: *Buildings for Nanoscale Research and Beyond*, San Diego, CA., 2005.
6 B. Bessason and C. Madshus, *Meas. Sci. Technol.*, 2000, **11**, 1527–1536.
7 F. B. Segerink, J. P. Korterik and H. L. Offerhaus, *Rev. Sci. Instrum.*, 2011, **82**, 065111.
8 J. R. Weaver, M. Voorhis and R. Reifenberger, *J. IEST*, 2009, **52**, 1–12.
9 H. Amick, B. Sennewald, N. C. Pardue, C. Teague and B. Scace, *Noise Contr. Eng.*, 1998, **46**, 39–47.
10 M. Banks, *Phys. World*, 2009, **10**, 6.
11 J. Bork, H.-D. Hahlbohm, R. Klein and A. Schnabel, *Biomag2000, Proceedings of the 12th International Conference on Biomagnetism*, 2001, pp. 790–794.
12 T. Brys, S. Czekaj, M. Daum, P. Fierlinger, D. George, R. Henneck, Z. Hochman, M. Kasprzak, K. Kohlik, K. Kirch, M. Kuznikak, G. Kuehne, A. Pichlmaier, A. Siodmok, A. Szelc and L. Tanner, *J. Res. Natl. Inst. Stand. Technol.*, 2005, **11**, 1.
13 A. Lassila, M. Kari, H. Koivula, U. Koivula, J. Korström, E. Leinonen, J. Manninen, J. Manssila, M. T. T. Meriläinen, J. Muttilainen, J. Nissilä, R. Nyblom, K. Riski, J. Sarilo and H. Isotalo, *Measurement*, 2011, **44**, 399–425.